Physica C 471 (2011) 250–257

Contents lists available at ScienceDirect

Physica C

journal homepage: www.elsevier.com/locate/physc

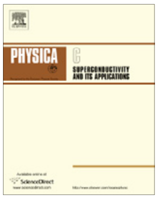

Interactions of $Ba_2YCu_3O_{6+x}$ with $SrTiO_3$ substrate

W. Wong-Ng [a,*], Z. Yang [a], J.A. Kaduk [b], L.P. Cook [a], S. Diwanji [a], C. Lucas [a]

[a] *Ceramics Division, Materials Science and Engineering Laboratory, National Institute of Standards and Technology, Gaithersburg, MD 20899, United States*
[b] *Poly Crystallography Inc., Naperville, IL 60540, United States*

ARTICLE INFO

Article history:
Received 20 December 2010
Received in revised form 7 February 2011
Accepted 9 February 2011
Available online 12 February 2011

Keywords:
Coated conductors
$Ba_2YCu_3O_{6+x}$ and $SrTiO_3$ interactions
Reaction products
Structure of $(Ba,Sr)_2RCu_3O_{6+x}$ (R = Pr, Nd, Sm, Eu, Gd, Dy, Ho, and Er)

ABSTRACT

This paper describes the crystal chemistry and crystallography of the products of reaction of $Ba_2YCu_3O_{6+x}$ with the $SrTiO_3$ buffer, which is a model system for coated conductors. A systematic study of the chemical interactions of $Ba_2YCu_3O_{6+x}$ and $SrTiO_3$ was conducted under 100 Pa p_{O2} (0.1% p_{O2}). The compounds determined based on the reactions of the bulk $Ba_2YCu_3O_{6+x}$ and $SrTiO_3$ include $(Ba,Sr)YTi_2O_{8.5}$, $(Ba,Sr)_2YCu_3O_{6+x}$, $(Ba,Sr)TiO_3$, $(Ba,Sr)_2TiO_4$, and CuO. The crystal structures of $(Ba,Sr)RTi_2O_{8.5}$ (R = Y and lanthanides), $(Ba,Sr)TiO_3$, $(Ba,Sr)_2TiO_4$, which have been previously reported, are reviewed. Detailed description of the $(Ba, Sr)_2RCu_3O_{6+x}$ (R = Pr, Nd, Sm, Eu, Gd, Dy, Ho, and Er) structure, as determined using X-ray Rietveld refinements, is given. Reference patterns of selected reaction products have been prepared and submitted to the Powder Diffraction File (PDF).

Published by Elsevier B.V.

1. Introduction

Continued world-wide research on high T_c superconductors has led to the promise of a wide variety of commercial applications, including improvements in electrical distribution grids, for more efficient utilization of energy resources. High-temperature superconductors have demonstrated potential for meeting these needs. Consequently, there has been an accelerated effort within the high T_c community on research and development of coated conductors for wire/tape applications [1–7]. For this application, $Ba_2YCu_3O_x$ (Y-213) and $Ba_2RCu_3O_x$ (R = lanthanides) are the principal superconducting materials. These superconductors can be deposited on flexible metallic tapes, and the resulting materials show excellent current-carrying capability.

The two principal state-of-the-art technologies for producing biaxially-textured substrates are Ion Beam Assisted Deposition (IBAD) [1,2], and Rolling Assisted Bi-axially Textured Substrate (RABiTS) [3–7]. This paper is relevant to the RABiTS architecture. Typically, a RABiTS film includes a number of buffer layers of different materials deposited on a biaxially grown metallic substrate. The general functions of these layers are to provide a physical/chemical barrier to substrate oxidation and substrate reaction with the superconductor layer and to provide texture for crystallographic alignment [8]. Examples of buffer layers applied to the substrate include CeO_2, $SrTiO_3$, Gd_3NbO_7, $LaMnO_3$, and $SrRuO_3$. Understanding interfacial reactions of $Ba_2YCu_3O_{6+x}$ with the buffer layers will provide information about how to control the formation of unwanted phases.

Previously we have reported the interfacial reactions of $Ba_2YCu_3O_{6+x}$ with CeO_2 [9,10], with Gd_3NbO_7 [11], and with $LaMnO_3$ [12]. This paper describes studies of the interaction of $Ba_2YCu_3O_{6+x}$ with $SrTiO_3$ in powder form, studies which will model the phases formed at the interface of a $Ba_2YCu_3O_{6+x}$ film and a $SrTiO_3$ substrate. Phase formation and structural studies of this system (and selected lanthanide-substituted systems) were conducted using X-ray diffraction and differential thermal analysis/thermal gravimetric analysis (DTA/TGA). As reference powder X-ray patterns are important for non-destructive phase analysis, selected patterns of the reaction products have been submitted for inclusion in the Powder Diffraction File (PDF) [13].

2. Experimental[1]

2.1. Preparation of samples in the $Ba_2YCu_3O_{6+x}$–$SrTiO_3$ system

A 10 g master batch of $Ba_2YCu_3O_{6+x}$ was prepared by heating a mixture of BaO, Y_2O_3 and CuO under purified air (CO_2- and H_2O-scrubbed). The BaO starting material was produced from $BaCO_3$ (99.99% purity, metals basis) by vacuum calcination in a vertical tube furnace. The following heating schedule was used: room temperature to 1300 °C in 20 h; isothermal at 1300 °C for 10 h; 1300 °C

---

* Corresponding author. Tel.: +1 301 975 5791.
E-mail address: winnie.wong-ng@nist.gov (W. Wong-Ng).

[1] Certain trade names and company products are mentioned in the text or identified in illustrations in order to adequately specify the experimental procedure and equipment used. In no case does such identification imply recommendation or endorsement by National Institute of Standards and Technology.

0921-4534/$ - see front matter Published by Elsevier B.V.
doi:10.1016/j.physc.2011.02.005

to room temperature in 20 h. To prepare $Ba_2YCu_3O_{6+x}$, stoichiometric amounts of BaO, Y_2O_3 and CuO were weighed, well-mixed and calcined in an atmospherically controlled high-temperature furnace first at 850 °C, then at 930 °C repeatedly with intermediate grindings for about 2 weeks.

A master batch of 10 g of $SrTiO_3$ was prepared by mixing stoichiometric amounts of TiO_2 and $SrCO_3$. The sample was heat treated at 750 °C, 900 °C, and 1200 °C with intermediate grindings for 1 week. Nine samples with different ratios of $Ba_2YCu_3O_{6+x}$: $SrTiO_3$ (10:90, 20:80, 30:70, 40:60, 50:50, 60:40, 70:30, 80:20, and 90:10) were prepared using the master $Ba_2YCu_3O_{6+x}$ and $SrTiO_3$ batches. Pelletized samples were placed inside individual MgO crucibles for annealing in a horizontal box-type controlled-atmosphere furnace. Transfer from the glove-box to the box furnace and vice versa was achieved via a transfer vessel and an interlock system attached to the furnace. Samples were annealed at 810 °C at p_{O2} = 100 Pa in air repeatedly until no further changes were observed in X-ray diffraction patterns. As the crystal structure of the x = 0, 0.2, 0.3, 0.4, 0.5 and 1.0 members of the $(Ba_{1-x}Sr_x)TiO_3$ solid solution has been reported in literature [14–19], phases of x = 0.6 and 0.8 members have been prepared to fill the gap of the $(Ba_{1-x}Sr_x)TiO_3$ series between x = 0.5 and x = 1.0. The x = 0.6 and 0.8 members were prepared in air at T = 1200 °C in air (mixing stoichiometric amounts of TiO_2, $BaCO_3$, and $SrCO_3$ followed by heat treatments at 750 °C, 950 °C, and 1200 °C with intermediate grindings).

Because it is likely that $Ba_2RCu_3O_{6+x}$ and $SrTiO_3$ have reaction products similar to the Y-analog, after identifying $(Ba,Sr)_3YTi_2O_{8.5}$ and $(Ba,Sr)_2YCu_3O_{6+x}$ as reaction products, two selected lanthanide-substituted solid solution series, namely, $Ba_3RTi_2O_{8.5}$ (R = Nd, Sm, Eu, Gd, Dy, Er, Tm, Yb, and Lu) and $(Ba,Sr)_2RCu_3O_{6+x}$ (R = La, Pr, Nd, Sm, Eu, Gd, Dy and Er) were also prepared in air for the study of their crystal chemistry. The $Ba_3RTi_2O_{8.5}$ series was prepared using stoichiometric amounts of $BaCO_3$, R_2O_3, and TiO_2. Heat treatments with intermediate grindings were carried out at 850 °C, 950 °C, 1100 °C and 1280 °C for R = Nd to Ho, and with further heat treatment to 1400 °C for R = Er to Lu. The $(Ba,Sr)_2RCu_3O_{6+x}$ series was prepared by mixing stoichiometric amounts of $BaCO_3$, $SrCO_3$, CuO and R_2O_3 and heat treated in air at 750 °C, 850 °C, 900 °C and 950 °C repeatedly. X-ray powder diffraction was used to identify the phases synthesized, to confirm phase purity, and to determine phase relationships.

2.2. Structural studies and reference X-ray powder diffraction patterns

Structure/reference patterns of reaction products were determined using the X-ray Rietveld refinement technique [20]. All data processing was carried out using GSAS [21]. For the $Ba_3RTi_2O_{8.5}$ series, the refinements included scale factors for the main and impurity phases and the lattice parameters. The heavy atoms were refined using individual isotropic displacement coefficients, while a common U_{iso} was refined for the oxygen atoms. Constraints were applied to the R–O and Ti–O bond distances. The peak profiles were described using the Thompson–Cox–Hastings pseudo-Voigt function including the Stephens model for anisotropic strain broadening (GSAS profile function #4). The strain and size broadening coefficients were refined. The small degrees of preferred orientation were modeled using 4th-order spherical harmonics. The backgrounds were described using 9-term shifted Chebyshev polynomials. Similar refinement strategies were followed for the other series of compounds.

For structural refinement of $(Ba,Sr)_2YCu_3O_{6+x}$, tetragonal *P4/mmm* and orthorhombic *Pmmm* structural models for $Ba_2YCu_3O_{6+x}$ were taken from the literature [22,23]. The impurity phases were also included using fixed structural models. For the refinement of the $(Ba_{1-x}Sr_x)TiO_3$ (x = 0.6 and 0.8) and the $Ba_3RTi_2O_{8.5}$ (R = Nd, Tm, and Lu) phases, the structure of $(Ba_{0.5}Sr_{0.5})TiO_3$ [18] and $Ba_3YTi_2O_{8.5}$ [24] were used as starting models, respectively.

Reference X-ray patterns of selected members $Ba_3RTi_2O_{8.5}$ (R = Nd, Tm, and Lu), $(BaSr)_2RCu_3O_{6+x}$ (R = La, Pr, Nd, Sm, Eu, Gd, Dy and Er), $(Ba_{2-x}Sr_x)TiO_4$ (x = 0.25, 0.5,0.75, and 1.0), and $(Ba_{1-x}Sr_x)TiO_3$ (x = 0.6 and 0.8) were prepared using a Rietveld pattern decomposition technique. These patterns represent ideal specimen patterns. They are corrected for systematic errors in both d and I. The reported peak positions are calculated from the refined lattice parameters, as these positions represent the best measure of the true positions. For peaks resolved at the instrument resolution function, the individual peak positions are reported. For overlapping peaks, the intensity-weighted average peak position is reported with multiple indices. For marginally-resolved peaks, individual peaks are reported to more accurately simulate the visual appearance of the pattern.

2.3. Differential thermal analysis/thermo-gravimetric analysis (DTA/TGA)

Simultaneous differential thermal analysis and thermo-gravimetric analysis (DTA/TGA) were used to study the melting events of the fully reacted samples with ratios of $Ba_2YCu_3O_{6+x}$:$SrTiO_3$ (10:90, 20:80, 30:70, 40:60, 50:50, 60:40, 70:30, 80:20, and 90:10). Most experiments utilized mainly the DTA signal; the TGA signal was useful primarily in following oxygen gain/loss associated with the CuO_x component. DTA/TGA experiments were performed using an electronically upgraded Mettler TA-1 system fitted with an Anatech digital control and readout system. The DTA/TGA apparatus was calibrated against the α/β quartz transition (571 °C) and the melting point of NaCl (801 °C), and temperatures reported in this study have a standard uncertainty of ±5 °C. Event temperatures were determined as the intersection of the baseline with the extrapolated linear portion of the rising DTA peak. Oxygen partial pressure during DTA/TGA was controlled using a previously analyzed Ar/O_2 mixture. During the experiments, gas was continuously flowed through the sample region at a rate of 150 ml/min, and the oxygen pressure at the outlet of the DTA/TGA system was periodically checked with a zirconia sensor.

3. Results and discussion

3.1. Reaction between $Ba_2YCu_3O_{6+x}$ and $SiTiO_3$

Fig. 1 summarizes the reaction products in three typical X-ray patterns at 810 °C and 100 Pa p_{O2}. The concentrations of product phases increase with increasing amounts of $SrTiO_3$. The phases present in all nine reaction products are the same, and only vary in concentration. These phases are $(Ba,Sr)_3YTi_2O_{8.5}$, $(Ba,Sr)_2YCu_3O_{6+x}$, $(Ba,Sr)TiO_3$, $(Ba,Sr)_2TiO_4$ and CuO. In summary:

$$Ba_2YCu_3O_{6+x} + SrTiO_3 \rightarrow (Ba,Sr)_3YTi_2O_{8.5} + (Ba,Sr)_2YCu3O_{6+x} + (Ba,Sr)TiO_3 + (Ba,Sr)_2TiO_4 + CuO$$

The above equation serves as a qualitative description of the reaction, and is not balanced, as the dopant quantity of Sr on the Ba site was not determined. $Ba_3YTi_2O_{8.5}$ has been reported by Derk et al. [25] to be the product of the reaction between $SrTiO_3$ and $Ba_2YCu_3O_{6+x}$. A small amount of Sr-doped Ba_2TiO_4 phase has also been observed at the interface of $SrTiO_3/Ba_2YCu_3O_{6+x}$ by Lu et al. [26].

The reaction products are in subsystems of the multi-component Ba–Sr–Y–Cu–Ti–O system. For example, $(Ba,Sr)_2YCu_3O_{6+x}$ is found in the Ba–Sr–Y–Cu–O system, which was described by Roth et al. [27]. Other phase diagrams of the pertinent subsystems in-